Integration Issues of Graphoepitaxial High-T_c SQUIDs Into Multichannel MEG Systems

M. I. Faley, I. A. Gerasimov, O. M. Faley, H. Chocholacs, J. Dammers, E. Eich, F. Boers, N. J. Shah, A. S. Sobolev, V. Yu. Slobodchikov, Yu. V. Maslennikov, V. P. Koshelets, and R. E. Dunin-Borkowski

Abstract—We have analyzed the possibility to construct multi-channel magnetoencephalography (MEG) systems based on high-T_c direct current superconducting quantum interference devices (DC SQUIDs) with graphoepitaxial step edge Josephson junctions. A new layout of multilayer high-T_c superconducting flux transformers was tested and a new type of high-T_c DC SQUID magnetometer intended for MEG systems was realized. These magnetometers have a vacuum-tight capsule of outer diameter 24 mm and a magnetic field resolution of $\sim$4 fT/$\sqrt{\text{Hz}}$ at 77 K. Crosstalk between adjacent sensors was estimated and measured for in-plane and axial configurations. The vibration-free cooling of sensors, minimization of the sensor-to-object distance and optimization of the sensor positions as well as the gantry design are discussed. Our findings may have implications for the next generation of non-invasive imaging techniques that will be used to understand human brain function.

Index Terms—Josephson junctions, magnetoencephalography, magnetometers, SQUIDs.

I. INTRODUCTION

THE IMPORTANCE of developing a new generation of non-invasive imaging techniques that can be used to understand human brain function is reflected, for example, in the "Human Brain Project" (EU) and the "BRAIN Initiative" (USA). Multichannel MEG systems that are based on low temperature SQUIDs are well developed and routinely used for the non-invasive investigation of multiple time-dependent sources of weak magnetic field generated by the human brain. MEG systems that are based on sensitive high-T_c SQUIDs promise to improve signal-to-noise ratio and to provide better source characterization by reducing the SQUID-to-scalp separation [1]. In a high-T_c system, one can achieve significant savings in energy and operational cost, in particular by avoiding problems with the supply of liquid helium [2], [3]. A single-channel MEG system based on high-T_c DC SQUID flip-chip magnetometers with a 16 mm $\times$ 16 mm multilayer flux transformer has achieved a magnetic field resolution of $\sim$4 fT/$\sqrt{\text{Hz}}$ at 77.4 K [4], [5], which is similar to the magnetic field resolution of individual channels in commercial MEG systems based on 28 mm $\times$ 28 mm low-T_c SQUIDs [6].

The magnetic signals that are detected by MEG originate from neocortical columns, each of which consists of $\sim$50 000 pyramidal cells with a net current $\sim$10 nA. The magnetic fields measured by MEG are $\sim$100 fT in the frequency range 1 Hz to 1 kHz. A spatial resolution of the MEG system of a few mm for such sources is usually sufficient. These values result in mutually dependent restrictions on the sensitivity, size and positioning of the SQUIDs: A reduction in the size of the sensors and in their proximity to the neural sources in the brain can partially compensate for a loss in sensitivity. On the other hand, more sensitive sensors allow for greater flexibility in the construction of the system. High-T_c SQUIDs can be cooled in cryostats that have fewer radiation shields and can be placed much closer to the outer wall than low-T_c SQUIDs. Assuming a similar field resolution and similar sizes of the sensors, the signal-to-noise ratio obtained during the detection of superficial and/or shallower sources of neuromagnetic signals by a high-T_c MEG system can be higher than for a low-T_c MEG system. At least 40% more information can be obtained using a high-T_c MEG system when compared to the state-of-the-art in low-T_c MEG systems [7].

The first source localization of brain activity using a single channel high-T_c system for MEG was demonstrated recently [8]. Taking into consideration possible systematic temporal drifts in the physiological and functional condition of the investigated brain area during the measurements, at least ten simultaneously operating channels are required for better diagnosis in practical applications of high-T_c MEG systems: for example, 7 signal channels and 3 reference channels. The construction of high-T_c MEG systems with more than 100 channels would be the next step in this development. However, multichannel high-T_c MEG systems have not yet been realized because of a number of issues associated with the integration of high-T_c SQUID magnetometers into the dense arrays of sensors that are required for MEG systems. Here, we describe these problems and suggest some solutions. First, we describe the properties of high-T_c SQUIDs that are essential for the construction of multichannel systems. Several issues, including crosstalk between the sensors, vibration-free cooling of sensors, minimization of the sensor-to-object distance, as well as optimization of the sensor positions and gantry design, are discussed.

II. HIGH-T_c SQUID MAGNETOMETERS

In a sufficiently magnetically well shielded room, it is preferable to use magnetometers instead of gradiometers for improved sensitivity to deep and/or distant sources. The magnetometers can be made fully with thin film technology, avoiding the use of superconducting wires. This results in comparable capabilities for high-T_c and low-T_c SQUIDs.

Multichannel high-T_c MEG systems comprise many high-T_c SQUIDs, some of which may require replacement over time. Although the technology required for producing low noise high-T_c SQUID magnetometers for MEG has been developed (see [5] and [9] and references therein), it is still not a mass production technology. Scaling to a higher production rate can be achieved by using parallel processing and/or larger single crystal MgO wafers, which are available in sizes of up to ~10 cm. High oxygen pressure sputtering allows deposition of large homogeneous areas of high-quality stoichiometric epitaxial heterostructures of superconducting cuprates with a mirror-like surface and superior electron transport properties [10]. The typical superconducting transition temperatures and critical current densities of $YBa_2Cu_3O_{7-x}$ (YBCO) films obtained by this method are ~93 K and ~$6 \cdot 10^6$ A/cm^2 at 77.4 K, respectively.

Epitaxial oxide thin-film heterostructures, including thin films of the superconductor $YBa_2Cu_3O_{7-x}$ (YBCO) have demonstrated a broad range of prospective applications. The further development of high-T_c superconducting devices is partially supported by the rapid development of metal-oxide heterostructures for applications such as room temperature resistive switching devices. We have observed large bipolar resistive switching in heterostructures that contain YBCO-$SrTiO_3$ interfaces, confirming results reported elsewhere [11]. Studies of the physical properties of epitaxial YBCO-$SrTiO_3$ heterostructures and other epitaxial heterostructures containing YBCO are essential for the production of low noise high-T_c SQUID magnetometers and gradiometers. For example, oxygen transport through epitaxial $SrTiO_3$ insulating films is important for resistive switching devices and for oxygenation of the bottom superconducting layer in multilayer high-T_c superconducting flux transformers.

The most suitable high-T_c SQUID magnetometers for multichannel systems from a price and quality point of view were recently developed [5]. These SQUIDs are based on high-T_c step-edge Josephson junctions, which are fabricated from specially oriented YBCO films grown on graphoepitaxially buffered steps on MgO substrates [9], [12]. The predecessors of such junctions were developed in the CSIRO group (see [13] and references therein). The cross-sectional areas of the graphoepitaxial junctions used in the SQUIDs are ~0.1 μm^2, which is about two orders of magnitude smaller than the cross-sectional area of typical Nb-based low-T_c junctions. Step edge junctions are also characterized by a larger normal state resistance $R_n \sim 20$ ohm, a higher I_cR_n of ~0.6 mV at 77.4 K and a lower capacitance C of ~10 fF, when compared to bicrystal high-T_c Josephson junctions [9]. The high resistance of these junctions leads to large voltage swings of the SQUIDs (by ~50 μV), but it promotes coupling to radio-frequency
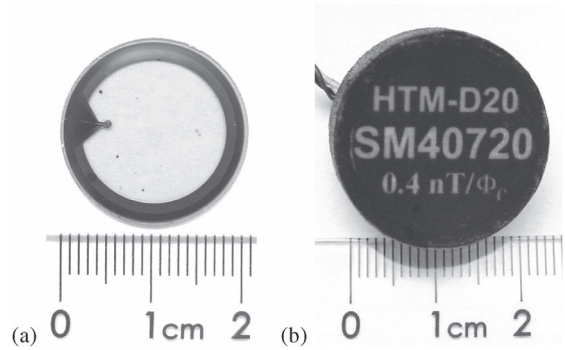

Fig. 1. (a) A multilayer high-T_c superconducting flux transformer with a 20 mm pick-up loop and a 14-turn input coil and (b) an encapsulated DC SQUID magnetometer containing such a flux transformer.

(RF) electromagnetic interference and results in the need for measures to achieve better RF filtering and shielding. The low capacitance of the Josephson junctions is advantageous for lowering the intrinsic flux noise of DC SQUIDs [14], [15]:

$$S_\Phi \approx 32 k_B T L \left(\frac{LC}{\beta_C} \right)^{\frac{1}{2}} \tag{1}$$

where $\beta_C = 2\pi I_C R_n^2 / \Phi_0 \approx 0.4$ is the McCumber parameter and $\Phi_0 = 2.07 \cdot 10^{-15}$ T $\cdot$ m^2 is the magnetic flux quantum. The lower operating temperatures of low-T_c SQUIDs are almost compensated by the typically much higher capacitance of their Josephson junctions (~1 pF). This property can explain the comparably high sensitivities of high-T_c and low-T_c SQUIDs in spite of the much higher operating temperature of high-T_c SQUIDs.

In MEG systems, near-optimal sensitivity of SQUIDs to magnetic fields can be provided by a superconducting flux transformer with a 14-turn input coil and a pick-up loop with an outer diameter of 20 mm. Fig. 1 shows a photograph of such a flux transformer and a vacuum-tight encapsulated high-T_c magnetometer (type HTM-D20) intended for assembly into a multichannel MEG system. The capsule has an outer diameter of ~24 mm, which is smaller than the 27-mm capsule for 16-mm magnetometers of type HTM-16 [16]. It encloses a flip-chip magnetometer, a feedback coil and a heater. The magnetometer consists of a 20 mm flux transformer that is inductively coupled to the high-T_c SQUID, as described in [5].

A schematic 3D layout demonstrating how the high-T_c SQUID, the superconducting flux transformer and modulation coil are coupled together is shown in Fig. 2. The 10-turn modulation and feedback coil has a diameter of 3 mm and is coupled to a 3 mm pick-up loop which is directly connected to the SQUID. The input coil of superconducting flux transformer is inductively coupled to 1 mm SQUID washer The magnetometer has a magnetic field sensitivity of ~0.4 nT/Φ_0 and a magnetic field resolution of ~4 fT/Hz at 77.4 K (see Fig. 3). The measurement of the noise spectrum was performed inside a 3-layer μ-metal shield and an YBCO superconducting shield.
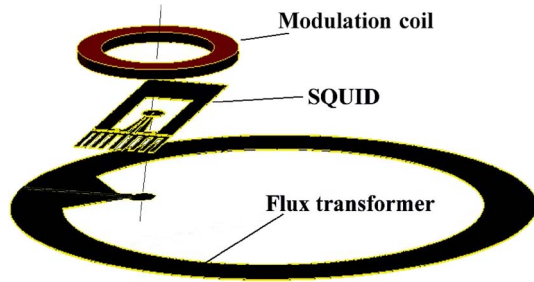
Fig. 2. A schematic 3D layout demonstrating how the high-T$_c$ superconducting flux transformer, the SQUID and modulation coil are coupled together.
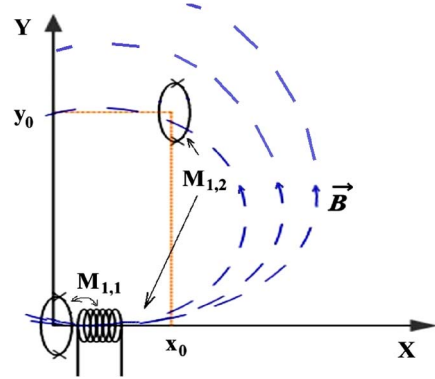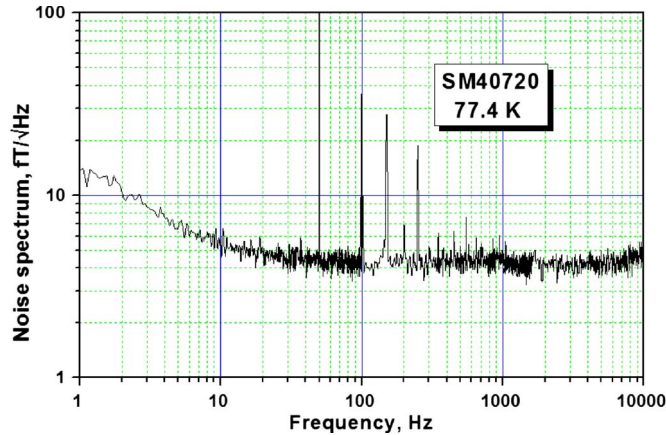

Fig. 3. Noise spectrum of an encapsulated magnetometer in a superconducting shield.

III. CROSSTALK BETWEEN HIGH-T$_c$ SQUID MAGNETOMETERS

In multi-channel SQUID systems, an important requirement is to prevent crosstalk between channels. Linearization of the output signal of each SQUID in a multichannel system is provided by modulation and feedback signals to each SQUID from its feedback coils. Parasitic inductive coupling between the feedback coil and the pick-up of the neighboring sensors should be minimized. Such coupling can be expressed in terms of crosstalk between the SQUID sensors in terms of the ratio between the flux induced by the feedback coil in a test sensor Φ_1 by a nearby inducing sensor and the flux read by the inducing sensor Φ_2:

$$\frac{\Phi_1}{\Phi_2} = \frac{M_{1,2}}{M_{1,1}} \approx \frac{\Phi_1^{pu}}{\Phi_2^{pu}} \tag{2}$$

where Φ_1^{pu} and Φ_2^{pu} are the fluxes in the pick-up loops of these two sensors, $M_{1,1}$ is the mutual inductance between the feedback coil and the sensing coil of the inducing SQUID and $M_{1,2}$ is the mutual inductance between the feedback coil of the inducing SQUID and the sensing coil of the test sensor (see Fig. 4).

Low crosstalk operation of SQUID arrays requires low values of $M_{1,2}$ and at the same time high values of $M_{1,1}$. The highest value of $M_{1,1}$ is generally provided by coupling the relatively large feedback coil to a pick-up loop that has a similar size, but in this case the value of $M_{1,2}$ is unacceptably high. With a fixed size of feedback coil, any increase in $M_{1,1}$ results

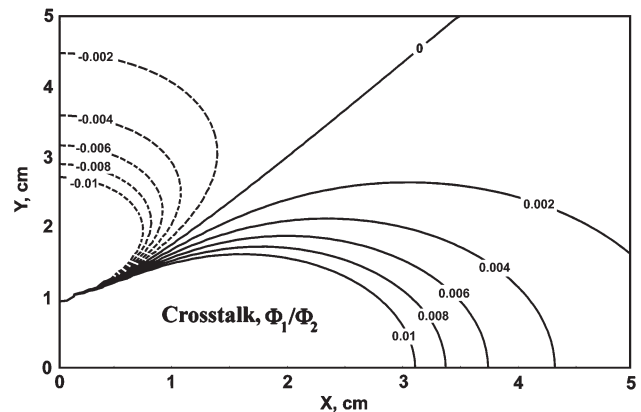Fig. 4. Schematic diagram of the setup for measuring crosstalk.

Fig. 5. Crosstalk calculation according to (4) and (5).

in an increase in $M_{1,2}$. In this work, we propose a 3-mm multi-turn feedback coil that is inductively coupled to a 3-mm direct coupled pick-up loop of the SQUID [5].

The feedback coil can be described as a magnetic dipole with a magnetic moment $|\vec{m}| = IN\pi r^2$ and a magnetic field

$$\vec{B} = \frac{\mu_0}{4\pi} \left[\frac{3(\vec{m}\vec{L})\vec{L}}{L^5} - \frac{\vec{m}}{L^3} \right] \tag{3}$$

where $\vec{L}$ is the distance from the dipole to the point of measurement, $\mu_0 = 4\pi \cdot 10^{-7}$ H/m, N = 10, and r = 1.5 mm is the radius of the feedback coil and the pick-up loop of the SQUID. The crosstalk is:

$$\frac{\Phi_1^{pu}}{\Phi_2^{pu}} \approx \frac{\mu_0 m}{4\pi \Phi_2^{pu}} \int_{y_0-R}^{y_0+R} \int_{-\sqrt{R^2-(y-y_0)^2}}^{\sqrt{R^2-(y-y_0)^2}} \frac{2x_0^2 - y^2 - z^2}{(x_0^2 + y^2 + z^2)^{\frac{5}{2}}} \, dz \, dy \tag{4}$$

where $R = 1$ cm is the radius of the pick-up loop of the neighboring magnetometer. The flux Φ_2 induced by the feedback coil in the pick-up loop of the inducing SQUID:

$$\Phi_2^{pu} \approx \frac{\mu_0 m r^2}{2 \left(r^2 + x_0^2 \right)^{\frac{3}{2}}}. \tag{5}$$

The result of the calculation of (4) and (5) is shown in Fig. 5, while experimentally measured data for Φ_1/Φ_2 are shown in Fig. 6.
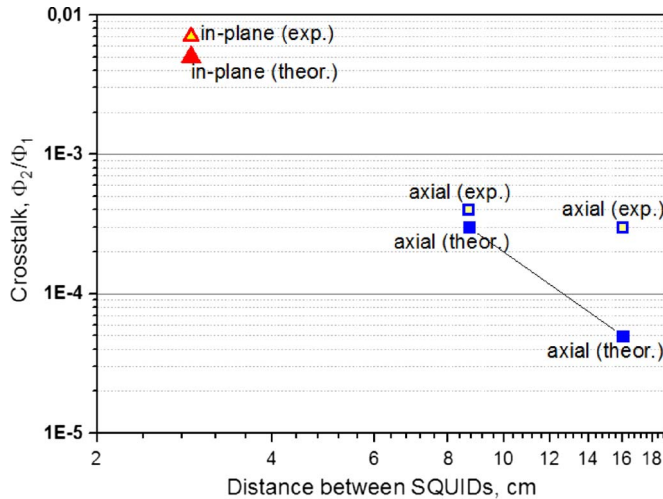
Fig. 6. Experimentally measured crosstalk for different positions of neighboring sensors and corresponding estimations: 1.) △,▲ for a coplanar orientation (along the Y-axis in Fig. 4) and 2.) □,■ for an axial orientation (along the X-axis).

Fig. 7. Example of positioning more than 100 encapsulated HTM-D20 magnetometers around a 3D model of the head of an adult human.

A crosstalk of below 1% was achieved at distances of more than 30 mm in both orientations. This measurement confirms the possibility to build close-packed arrays of high-T_c SQUID magnetometers with the proposed configuration of feedback coil.

IV. INTEGRATION OF SENSORS INTO MULTICHANNEL HIGH-T_c MEG SYSTEMS

To take full advantage of high-T_c SQUIDs, they should be placed in a dense array as close as possible to the scalp and to neighboring sensors. More than 100 encapsulated HTM-D20 magnetometers can be arranged around the head of an adult human (see Fig. 7). The problem is the variety of individual sizes of heads that should be accommodated in a mechanically adjustable MEG system to maintain close proximity of the sensors to the scalp.

In principle, each channel can be placed in an individual cryostat with a small area at its lower end and individually adjusted to the scalp [17]. The advantage of such a segmented
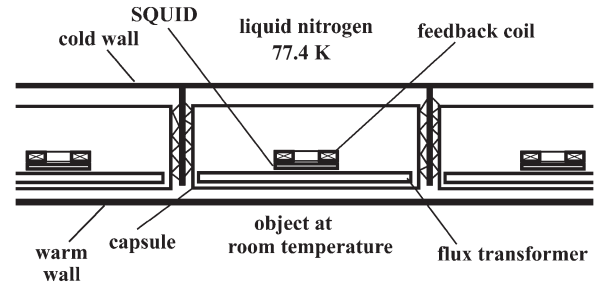

Fig. 8. Schematic view of an array of HTM-D20 magnetometers cooled siDewards in the vacuum space of a liquid nitrogen cryostat.

helmet construction is the possibility to realize a SQUID-to-scalp separation down to ∼3 mm by using a very thin wall at the bottom end of a small cryostat. The main disadvantage is the increased tangential separation between the channels due to the sidewalls of the cryostat, leading to the attenuation of high spatial frequencies in the MEG signals. Multiple cryogen transfers and cryostat costs are less critical for high-T_c systems when compared to the low-T_c systems suggested in [17]. One can use, for example, a single central reservoir with a solid and liquid nitrogen mixture at a triple point temperature of 63.15 K and flexible leads for controlled temperature transfer to the sensors of the individual channels. This approach would solve the problem of vibration-free cooling of the sensors, which is especially important for MEG systems.

Another approach is to use several multi-channel systems with individual cryostats with near-flat bottom ends. Each cryostat can then enclose, for example, 7 signal channels, as achieved in a dual seven-channel MEG system from Biomagnetic Technologies, Inc. (see Fig. 2 in [18]). Such a configuration can be used for small region recording and can have advantages in spatial resolution when compared to a low-T_c MEG system and a high resolution EEG system [19].

The high-T_c sensors may be placed very close (< 3 mm) to the scalp by locating them in the vacuum space of the cryostat, as shown schematically without maintaining the relative dimensions in Fig. 8. In this case, the sensors are fixed inside thermal conducting sockets and cooled sidewards for example with the help of vacuum grease. The thermal radiation shields between the sensors and the warm wall are not shown here. Alternatively, the sensors can be placed inside individual dimples on the other side of the cold wall, preferably immersed in liquid nitrogen.

When constructing the cryostat holder or gantry for a multichannel high-T_c MEG system, one should take into account that the density of liquid nitrogen (∼0.8 kg/liter) is much higher than that of liquid helium (∼0.128 kg/liter). A typical 50 liter cryostat for MEG would be ∼33 kg heavier if it would be filled with liquid nitrogen. This may require modifications of contemporary gantries for low-T_c MEG systems.

REFERENCES

[1] F. Öisjöen *et al.*, "High-T_c superconducting quantum interference device recordings of spontaneous brain activity: Towards high-T_c magnetoencephalography," *Appl. Phys. Lett.*, vol. 100, no. 13, Mar. 2012, Art. ID. 132601.

[2] M. Peplow, "US bill would keep helium store afloat," *Nature*, vol. 497, no. 7448, pp. 168–169, May 2013.

[3] J. Good, "Comment: Solving the liquid helium problem," *Mater. Today*, vol. 17, no. 1, pp. 2–3, 2014.

[4] M. I. Faley, U. Poppe, K. Urban, D. N. Paulson, and R. L. Fagaly, "A new generation of the HTS multilayer DC-SQUID magnetometers and gradiometers," in *J. Phys.: Conf. Ser.*, 2006, vol. 43, pp. 1199–1202.

[5] M. I. Faley *et al.*, "High-T_c DC SQUIDs for magnetoencephalography," *IEEE Trans. Appl. Supercond.*, vol. 23, pt. 1, no. 3, Jun. 2013, Art. ID. 1600705.

[6] "Elekta Neuromag System Hardware," *Technical Manual, Revision F*, 2005.

[7] J. F. Schneiderman, "Information content with low- vs. high-T_c SQUID arrays in MEG recordings: The case for high-T_c SQUID-based MEG," *J. Neurosci. Methods*, vol. 222, pp. 42–46, Jan. 2014.

[8] J. Dammers *et al.*, "Source localization of brain activity using helium-free interferometer," *Appl. Phys. Lett.*, vol. 104, no. 21, 2014, Art. ID. 213705.

[9] M. I. Faley, D. Meertens, U. Poppe, and R. E. Dunin-Borkowski, "Graphoepitaxial Josephson junctions and DC SQUIDs," in *Proc. 14th ISEC*, 2013, pp. 1–3.

[10] U. Poppe *et al.*, "Low-resistivity epitaxial YBa$_2$Cu$_3$O$_{7-x}$ thin films with improved microstructure and reduced microwave losses," *J. Appl. Phys.*, vol. 71, pp. 5572–5578, 1992.

[11] K. Li, Z. Wen, D. Wu, H. Zhai, and A. Li, "Bipolar resistive switching based on SrTiO$_3$/YBa$_2$Cu$_3$O$_7$ epi-layers," *J. Phys. D: Appl. Phys.*, vol. 46, no. 3, Jan. 2013, Art. ID. 035308.

[12] M. I. Faley, "Reproduzierbarer Stufen-Josephson-Kontakt," Patent DE 102012006825 A1 (10.10.2013).

[13] E. E. Mitchell and C. P. Foley, "YBCO step-edge junctions with high $I_c R_n$," *Supercond. Sci. Technol.*, vol. 23, no. 6, Jun. 2010, Art. ID. 065007.

[14] J. Clarke, "SQUID fundamentals," in *SQUID Sensors: Fundamentals, Fabrication Appl. (NATO ASI Series E: Applied Science. 329)*, H. Weinstock, Ed. Dordrecht, The Netherlands: Kluwer Academic, 1996, pp. 1–62.

[15] M. Schmelz *et al.*, "Highly sensitive miniature SQUID magnetometer fabricated with cross-type Josephson tunnel junctions," *Physica C*, vol. 478, pp. 77–80, Jun. 2012.

[16] M. I. Faley *et al.*, "Low noise HTS dc-SQUID flip-chip magnetometers and gradiometers," *IEEE Trans. Appl. Supercond.*, vol. 11, no. 1, pp. 1383–1386, Mar. 2001.

[17] A. Matlashov, A. Bakharev, Y. Zhuravlev, and V. Slobodchikov, "Biomagnetic multi-channel system consisting of several self-contained autonomous small-size units," in *Supercond. Devices Their Appl.*, vol. 64, H. Koch and H. Lübbig, Eds. Berlin, Germany: Springer-Verlag, 1992, pp. 511–516.

[18] R. L. Fagaly, "Neuromagnetic instrumentation," in *Adv. Neurology, vol. 54: Magnetoencephalography*, S. Sato, Ed. New York, NY, USA: Raven Press, 1990, pp. 11–32.

[19] J. Malmivuo, "Comparison of the properties of EEG and MEG in detecting the electric activity of the brain," *Brain Topography*, vol. 25, pp. 1–19, 2012.